sustainability

MDPI

Article

Spatiotemporal Dynamics and Driving Factors of Ecosystem Services Value in the Hexi Regions, Northwest China

Yongge Li [1,2], Wei Liu [1,*], Qi Feng [1], Meng Zhu [1], Jutao Zhang [1], Linshan Yang [1] and Xinwei Yin [1]

[1] Key Laboratory of Ecohydrology of Inland River Basin, Qilian Mountains Eco-Environment Research Center in Gansu Province, Northwest Institute of Eco-Environment and Resources, Chinese Academy of Sciences, Lanzhou 730000, China
[2] University of Chinese Academy of Sciences, Beijing 100049, China
* Correspondence: weiliu@lzb.ac.cn

Abstract: Land-use and climate changes can exert significant influences on ecosystem services value (ESV). However, interactions of these drivers in shaping the ESV remain unclear in arid inland regions. In this study, dynamic changes in ESV from 1980 to 2050 in the Hexi Regions were evaluated by integrating land-use change and other environmental factors using the equivalent factor method, local spatial autocorrelation analysis, and a geographical detector. Our results showed that the spatial distribution of ESV increased in the northwest to southeast regions of the study area. The area-weighted mean ESV of the Qilian Mountains (i.e., mountainous regions) was about 10.27–11.97-fold higher than that of the Hexi Corridor (i.e., plain regions) during the study period. As for the ecological protection (EP) scenario, from 2020 to 2050, the total ESV increase was estimated to be larger than that under the natural development (ND) and rapid urbanization (RU) scenarios. Particularly, under the EP scenario, by 2050, the enhancement of ESV in the Qilian Mountains mainly resulted from the expansion of forests, shrubs, grasslands, and water. The geographical detector indicated that LUCC was the dominant driver of the spatial heterogeneity of ESV, followed by climate and vegetation. Specifically, LUCC explained 35.39% and 80.06% of the total variation in the ESV for the Hexi Corridor and the Qilian Mountains, respectively. Natural drivers, such as temperature, precipitation, evapotranspiration, and soil organic carbon, were assumed to exert larger impacts on ESV in the mountainous regions than in the corridor. By contrast, anthropogenic factors played more significant roles in altering the ESV patterns for the corridor. Our research highlighted the importance of ecological protection in improving ESV in the future and emphasized that the difference in driving factors of ESV between mountainous and plain regions should be considered in terms of the ecosystem management for the inland regions of northwestern China.

Keywords: LUCC simulation; ecosystem services values; spatiotemporal dynamics; driving factors

Citation: Li, Y.; Liu, W.; Feng, Q.; Zhu, M.; Zhang, J.; Yang, L.; Yin, X. Spatiotemporal Dynamics and Driving Factors of Ecosystem Services Value in the Hexi Regions, Northwest China. *Sustainability* **2022**, *14*, 14164. https://doi.org/10.3390/su142114164

Academic Editors: Alimujiang Kasimu and Liwei Zhang

Received: 5 October 2022
Accepted: 27 October 2022
Published: 30 October 2022

1. Introduction

Ecosystem services are the potential benefits that human obtained from both natural and artificial ecosystems [1], mainly consisting of provisioning, regulating, supporting and cultural services [2], which affect human well-being (e.g., basic material, health, security, freedom of choice, and action) [3]. The ecosystem services value (ESV) was used to quantify the economic value of ecosystem services and functions using economic analysis with monetary values [4,5], which can mitigate the growing scarcity of ecosystem services, ensuring effective ecosystem management and scientific decision making [5,6]. For example, phytoplankton, an ecosystem engineer, has greatly promoted biogeochemical cycles and nutrient cycling in aquatic and terrestrial ecosystems, providing fundamental services (e.g., oxygen production, nutrient cycling, food, fuels, and drugs) for life to create direct and indirect economic value [7]. Over the past decades, research has shown that the functions and values of ecosystem services have degraded due to climatic and land-use

changes [8–10]. Recently, the land use and land cover change (LUCC) has been more frequent on the global and regional scales [11,12], and these land conversions may lead to land degradation (e.g., soil erosion, salinization, desertification) [13], biodiversity decline, and the loss of ecosystem services [14,15], which in turn affects food and ecological security. Most studies have suggested that the land-use changes may exert negative impacts on the ESV associated with inappropriate human exploitation [16] and the complex interactions between human and natural drivers of the ESV, rendering the previous studies insufficient for predicting and addressing future problems. In order to further reduce ecological risk, maintain the essential ecosystem functions, and achieve sustainable development goals, we should explicitly explore the potential relationships between the ESV and environmental controls, determining the interactive mechanisms of multiple controls under multi-scenario simulations.

The estimation of ESV will enable us to better measure natural capital, making nature's values visible; thus, the importance of protecting the ecological environment in terms of sustainable resource utilization and biodiversity conservation protection will be more significant for the public and policy-makers [8,17]. At present, there have been numerous studies assessing the ESV; common methods include the ecological model method [18,19] and the equivalent factor method [20,21]. Ecological models such as the Multiscale Integrated Model of Ecosystem Services (MIMES) [22] and the Integrated Valuation of Ecosystem Services and Tradeoffs (InVEST) model [23], were applied to calculated ecosystem functions and the ESV based on spatially explicit gridded data. Compared with ecological models, the equivalent factor method was widely used to assess the comprehensive ESV on the regional or global scale by assigning monetary values to different land-use types [16,24].

However, previous research focused more on the evaluation of the historic ESV and its driving factors. Due to the uncertainties and complexities of climate change, less attention was paid to the future ESV estimation according to different climate and land-use change scenarios. The commonly used methods to simulate land-used changes and the ESV include the Markov chain [25], cellular automata (CA), CA-Markov chains [26], the conversion of land use and its effects (CLUE-S) model [27], geographical simulation and optimization system (GeoSOS) [28], the future land use simulation (FLUS) model [29], artificial neural networks, mixed-cell CA models [30], and the patch-generating land use simulation (PLUS) model [31]. Compared to other models, the PLUS model could efficiently simulate the spatiotemporal dynamics of different land-use category conversions based on the combination of CA models and land expansion analysis [32]. In addition, interactions among ecosystem services due to policy interference and environmental changes may cause a change in one service that alters another, including trade-offs in a competitive relationships, and the fact that synergies can refer to an increase or decrease simultaneously [33]. For example, the Grain to Green Program (GTGP) has enhanced the synergistic relationships among soil conservation, habitat quality, and carbon sequestration over the head regions of the Yangtze River, increasing trade-offs between these services and food production and water yield [34]. Correlation analysis, spatial autocorrelation, and scenario analysis have been common methods used for evaluating the relationships among ecosystem services [35,36].

The Hexi Regions, as typical arid inland regions, consist of mountain-oasis-desert landscapes [37], which are vulnerable to climate change and human disturbances [38]. Over the past decades, climate change and inappropriate activities have resulted in numerous environmental issues in the Hexi Regions, such as the shrinkage of glaciers, coal mining and hydropower station expansion, grassland degradation, and desertification [39,40], which have raised more concerns from governments, scholars, and the public. Currently, most studies focus on the changes and drivers of historical ecosystem services and ESV on a local scale [41], such as administrative boundaries or small basins, to some extent, ignoring ecosystem integrity across all the Hexi Regions. Meanwhile, there are relatively few studies regarding the effects of interaction among drivers of ESV. A comprehensive analysis of the ESV and its environmental controls over the past and in the future is needed to ensure effective management of ecosystem services and scientific decision making for inland

regions. Therefore, this study aims to: (1) quantify the patterns of ESV based on multiple land-use change scenarios and the equivalent factor method, (2) to identify trade-offs and synergies among ecosystem services based on ESV, and (3) to determine the main drivers of ESV using the geographical detector.

2. Materials and Methods

2.1. Study Area

The Hexi Regions are located in northwestern China, consisting of the Qilian Mountains (i.e., mountainous regions, 2000–5838 m a.s.l) and the Hexi Corridor (i.e., plain regions, altitude 660–2000 m a.s.l), covering an area of 3.80×10^5 km^2 (Figure 1). The Hexi Corridor, characterized by lower elevation and flat terrain, is a series of oases with concentrated populations and well-developed irrigated agriculture in the Hexi Regions [42]. The modern glaciers in the Qilian Mountains supply large amounts of fresh water to the Hexi Corridor [43], assuring the developments of oases. The mean annual temperature and precipitation range from −12 to 12 °C and 50 to 700 mm, respectively [44]. The precipitation is mostly concentrated in the mountains, and decreases significantly from the east to west of the study area. The landscapes exhibit significant vertical zonality, with vegetation types varying from alpine desert, alpine and subalpine grassland, shrubland, forest, steppe, desert steppe, to Gobi desert [45]. In addition, due to the arid climate, the dominant land cover types are bare lands, low-cover grasslands, and sandy lands (Figure 2). Moreover, the forests, shrublands, and grasslands (including high-, medium- and low-cover grasslands) are mainly distributed in the east Qilian Mountains, and cropland is primarily located in the valleys of mountains and the oases of the Hexi Corridor.

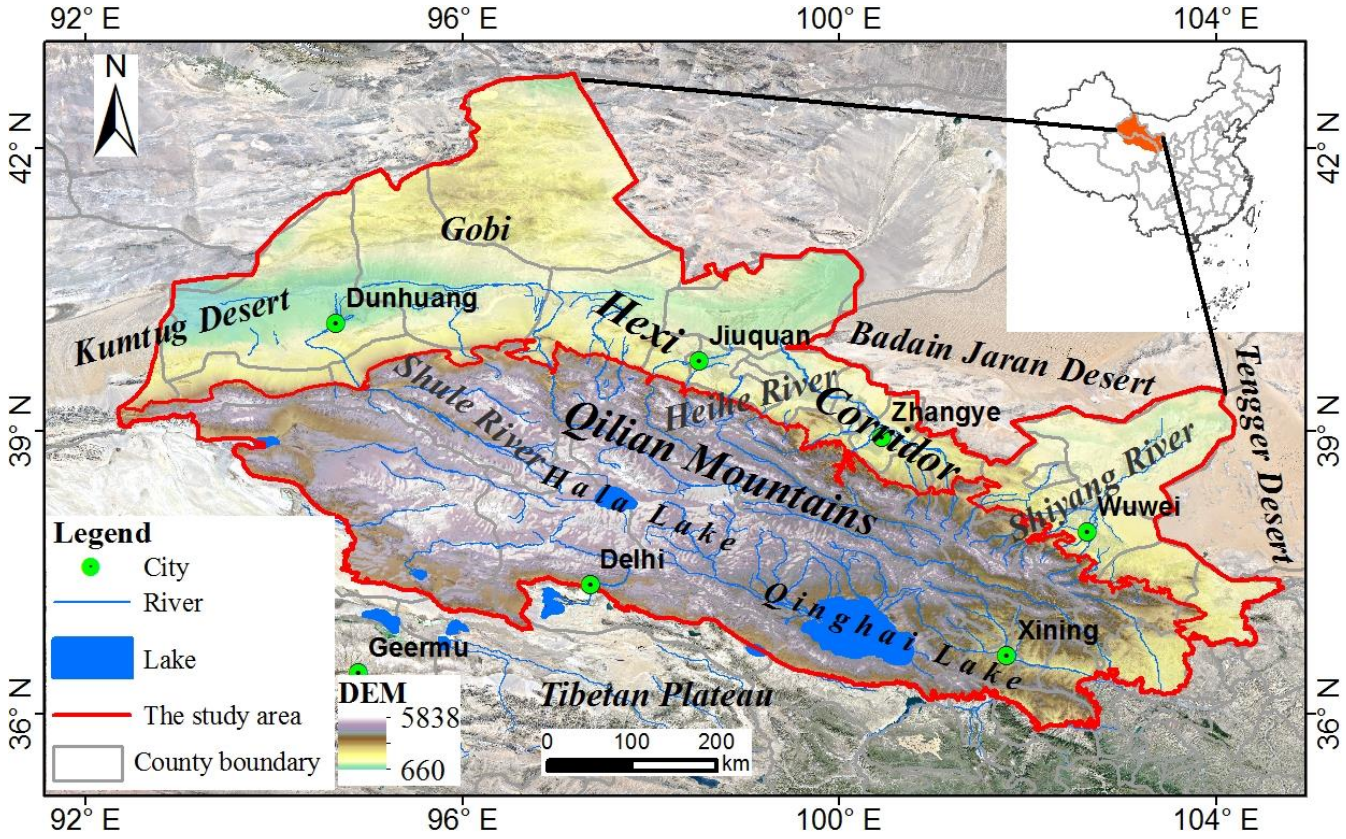

Figure 1. Locations of the study area.

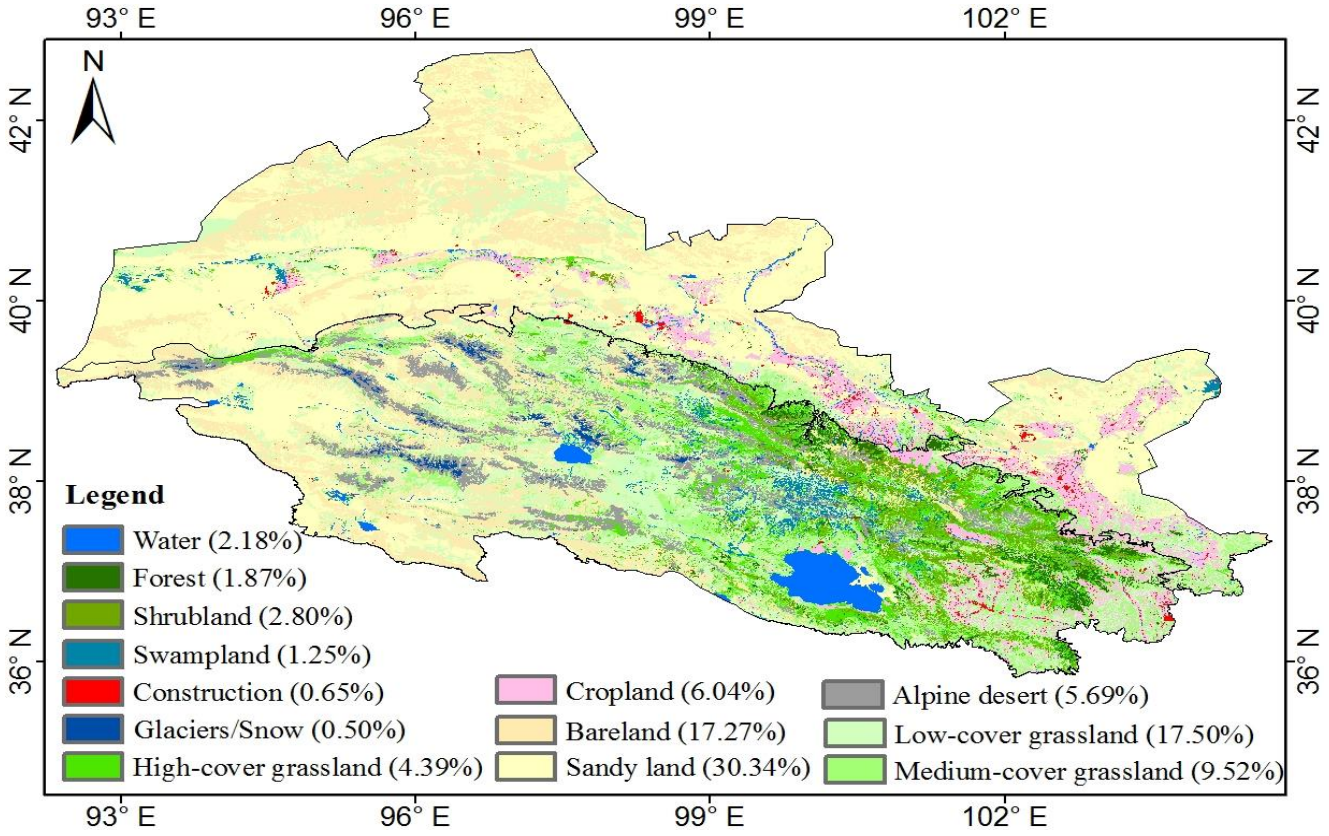

Figure 2. The spatial distribution of land cover types in the Hexi Regions (2020).

2.2. Data Sources

We used land use and land cover change (LUCC), topography, climate, soil, vegetation, and socio-economic data (e.g., county points, population, and roads) for further analysis (Table 1). The LUCC datasets for 1980–2020, at 10-year intervals, were used, including those for 1980, 1990, 2000, 2010, and 2020. To obtain higher accuracy, the gridded dataset was spatially downscaled from the 0.5° population and the GDP dataset with 1 km and the RESDC dataset using delta spatial downscaling [46]. Additionally, grain datasets including the price, yield, and area of potatoes, canola, wheat, and corn were derived from the National Compendium of Agricultural Product Cost and Benefit Information (1985–2020) and the National Bureau of Statistics in China (http://www.stats.gov.cn/ (accessed on 20 July 2022).

Table 1. The environment variables used for exploring the drivers of ESV.

Type	Variables (Resolution)	Source
LUCC	1980–2020 LUCC datasets (1 km)	The Data Center for Resources and Environmental Sciences, Chinese Academy of Sciences (RESDC) (http://www.resdc.cn (accessed on 10 March 2022)).
Topography	Elevation (30 m) Surface roughness (30 m) Slope (30 m)	Geospatial Data Cloud (http://www.gscloud.cn (accessed on 23 June 2021)). The slope and surface roughness were obtained from the elevation data.
Climate	1980–2020 Potential evapotranspiration (1 km)	Potential evapotranspiration (1980–2020) was calculated by the Penman–Monteith equation with meteorological data from the China Meteorological Data Service Center (CMDC) (http://data.cma.cn/ (accessed on 23 June 2021)) [47].
	1901–2100 Temperature dataset (1 km) 1901–2100 Precipitation dataset (1 km)	1 km monthly temperature and precipitation dataset for China from 1901–2100 [46,48,49] (http://data.tpdc.ac.cn (accessed on 10 May 2022)).
Vegetation	2000–2020 NPP (500 m)	The U.S. Geological Survey (USGS) and the National Aeronautics and Space Administration (NASA) (https://lpdaac.usgs.gov/ (accessed on 20 July 2022)).

Table 1. *Cont.*

Type	Variables (Resolution)	Source
	1986–2020 NDVI (30 m)	National Tibetan Plateau Data Center (http://data.tpdc.ac.cn (accessed on 23 June 2021)). The fractional vegetation coverage was calculated using the NDVI dataset.
Soil	2018 Soil organic carbon density (30 m)	National Cryosphere Desert Data Center [50] (http://www.ncdc.ac.cn (accessed on 30 September 2021)).
Traffic network	2015 Road density (1:1 million)	National Basic Geographic Database (https://mulu.tianditu.gov.cn/ (accessed on 25 June 2021)).
County points data	2015 Distance to settlement (1:1 million)	
Population	1990–2100 Population (POP)	The GDP and POP gridded dataset at 1 km and 0.5° resolution were acquired from the Resources and Environment Science Data Center of the Chinese Academy of Sciences (RESDC) (http://www.resdc.cn/ (accessed on 25 June 2021)) and Science Data Bank [51] (http://cstr.cn/31253.11.sciencedb.01683 (accessed on 15 May 2022)), respectively.
Economy	1990–2100 Gross Domestic Product (GDP)	

2.3. Methods

2.3.1. Estimation of the ESV

This study used the method of equivalent value factor per unit area to evaluate the ESV. The method was modified and developed by Chinese scholars based on a literature survey, expert knowledge, and multi-source data [52], which was suitable for the evaluation of ESV in China [26]. The ESV of the Hexi Regions is calculated using the formula:

$$\mathrm{ESV} = \sum_{i=1}^{n} A_i \times VC_i \tag{1}$$

$$VC_i = \sum_{j=1}^{k} EC_j \times E_a \tag{2}$$

where ESV is the total of ecosystem services value (CNY); i is the type of land use; j is the type of ecosystem services; A_i is the area of land use type i (hm^2); VC_i is the per unit area of ESV in the land use type i ($\mathrm{CNY \cdot hm^{-2} \cdot yr^{-1}}$); EC_j is the value equivalent of ESV of ecosystem service j for the land use i; and E_a is the economic value of 1 unit of ESV ($\mathrm{CNY \cdot hm^{-2} \cdot yr^{-1}}$). In order to more accurately obtain E_a in the Hexi Regions, combined with the field situation, we mainly consider four grains (i.e., wheat, corn, potatoes, and canola) [26]:

$$E_a = \frac{1}{7} \sum_{w=1}^{s} \frac{m_w p_w q_w}{M} \tag{3}$$

where E_a is the economic value of 1 unit of ESV; w is the type of food; m_w is the average price of the w grain; p_w is the yield of w food; q_w is the planting area of the w food; and M is the total planted area of the food. The multi-year price of the four grains was used for calibration, and the results showed that the economic value of unit ESV in the Hexi Regions was 1367.30 $\mathrm{CNY \cdot hm^{-2} \cdot yr^{-1}}$.

2.3.2. Land Use Simulation

We employed the PLUS model to simulate LUCC by combining the land expansion analysis strategy and a CA model on the basis of multitype random seeds [32]. The models extracted the various types of land use expansion between two periods of LUCC and detected the drivers of LUCC using the random forest algorithms, generating the growth probability $P_{c,k}^{d}$ of land-use type k at cell c [32]:

$$P_{c,k}^{d}(x) = \frac{\sum_{n=1}^{M} I(h_n(x) = d)}{M} \tag{4}$$

where $P_{c,k}^{d}$ indicates the growth probability of land-use type k in cell c, the d value is either 0 or 1; x is a vector of multiple drivers; $I(\cdot)$ refer to the indicative function for the decision tree set, $h_n(x)$ represents the prediction type of the n–th decision tree for vector x, and M represents number of decision trees.

The CA model calculated the overall probability according to the following formula [32]:

$$OP_{c,k}^{d=1,t} = \begin{cases} P_{c,k}^{d=1} \times (r \times \mu_k) \times D_k^t \; if \; \Omega_{c,k}^t = 0 \; and \; r < P_{c,k}^{d=1} \\ P_{c,k}^{d=1} \times \Omega_{c,k}^t \times D_k^t \; all \; others \end{cases} \quad (5)$$

where $OP_{c,k}^{d=1,t}$ represents the overall probability of the land-use type k; $P_{c,k}^{d=1}$ represents the growth probability of land-use type k at cell c; D_k^t represents the impact of the future demand for land-use type k; $\Omega_{c,k}^t$ is the neighborhood effects of cell c; r is a random value from 0 to 1; μ_k indicates the threshold for generating new land use patches of land use type k. More details regarding the PLUS software are available at https://github.com/HPSCIL/Patch-generating_Land_Use_Simulation_Model (accessed on 15 August 2021).

To analyze and detect the ESV changes under different future scenarios of LUCC, we developed three potential LUCC scenarios, namely natural development (ND), ecological protection (EP), and rapid urbanization (RU). The ND scenario was developed based on the historical trend of LUCC, and the EP scenario emphasized the protection of ecological land (e.g., the forest, grassland, and water) and the restriction of construction land expanded to ensure sustainable development. The RU scenario prioritized economic development with the intense use of fossil fuels, leading to the expansion of construction land.

The future projections of temperature, precipitation, population, and GDP were employed to simulate the LUCC trend [44]. The four factors were derived from the latest Coupled Model Intercomparison Project Phase 6 (CMIP6) model, which coupled shared socioeconomic pathways (SSPs) and representative concentration pathways (RCPs) [53]. Different scenarios corresponded to different factor combinations; the corresponding temperature, precipitation, population, and GDP data for EP, ND, and RU scenarios are SSP1 and RCP2.6 (SSP1-2.6), SSP2 and RCP4.5 (SSP2-4.5), and SSP5 and RCP8.5 (SSP5-8.5), respectively [54].

Additionally, the kappa coefficient was used to test the performance of the PLUS model. A credible model was assumed to act with a kappa coefficient larger than 0.80 [44]. Relevant drivers involved in LUCC simulations can be found in our previous research results [44]. Based on the LUCC data and driving factors from 2000 to 2010, we simulated and predicted the LUCC in 2020. Compared with the actual LUCC in 2020, we found that the kappa coefficient was greater than 0.87, indicating that PLUS can be used to simulate LUCC in this study area. On this basis, we used the PLUS model to simulated the dynamics of LUCC in 2050 based on land use data from 1990 to 2020. The spatial distribution of LUCC during the study period is shown in Figure S1 in the Supplementary Materials, and land use and land transfer are shown in Figures S2 and S3 in the Supplementary Materials.

2.3.3. Trade-Offs and Synergies Analysis Method

We applied the Pearson correlation analysis coefficient to explore the synergistic and trade-off relationships between ecosystem services based on the ESV; positive and negative correlations implied synergistic and trade-off relationships between paired ESV, respectively, and the p value detected significant differences between paired ESV; ** means significance at the $p < 0.01$ level [55].

The local indicators of spatial association (LISA), a type of local spatial autocorrelation analysis, was also known as the Local Moran's I [56], including univariate and bivariate Local Moran's I. Bivariate Local Moran's I was a particularly effective tool for exploring and modeling spatial patterns of different geographical elements [57,58]. More specifically, the bivariate Local Moran's I analysis generated four different types of spatial clusters; high-high and low-low clusters indicated synergistic relationships between paired ESV; high-low and low-high clusters indicated trade-off relationships between paired ESV, and the above four clusters were significant at $p = 0.05$; non-significance implied that no obvious trade-off or synergistic relationships existed [37]. In order to reveal the heterogeneity of trade-off and synergistic relationships among ecosystem services based on the ESV in

the Hexi Regions, we employed this method-based GeoDA software (http://geodacenter.github.io/download.html (accessed on 20 July 2022)).

2.3.4. Geographical Detector Analysis

The geographical detector was utilized to measure the spatial stratified heterogeneity (SSH) among variables [59], and to detect the explanatory power of each control (explanatory variables x) accountable for the dependent variable Y in the heterogeneity based on consistency between their spatial distributions [60], as well as to investigate the interaction between two explanatory variables with a dependent variable, including the strength, direction, and linearity or nonlinearity. The geo-detector was not affected by a linear hypothesis compared to the traditional linear model and possessed a definite physical meaning [60,61]. In this study, the ESV was used as the dependent variable, and environmental factors were used as the independent variables. In order to identify the factors that have a decisive impact on the ESV and to reveal whether these factors interact with each other or independently contribute to the ESV in the Hexi Regions, we employed the factor detector and interaction detector to evaluate the impact of each driving factor (x_i) on the ESV on the basis of the q-statistic value; the formula is as follows [60]:

$$q(x_i) = 1 - \frac{\sum_{h=1}^{L} N_h \sigma_h^2}{N\sigma^2} = 1 - \frac{SSW}{SST} \tag{6}$$

$$SSW = \sum_{h=1}^{L} N_h \sigma_h^2,\ SST = N\sigma^2 \tag{7}$$

where $q(x_i)$ is q-statistic value, indicating the explanatory power of environmental factors(x_i) on the ESV in the study area, with a value between 0 and 1, and the larger $q(x_i)$ indicates the stronger effect of x_i on the ESV; h (1, . . . , L) is the number of strata of a driving factor x; N is the total number of units of the ESV; σ^2 is the variance of the ESV; N_h represents the number of units in strata h; σ_h^2 is the variance of the ESV in strata h; SSW and SST refer to the within sum of squares and the total sum of squares, respectively.

The q-statistic value was generally used to detect spatial stratified heterogeneity and to determine the interactive relationships among environmental controls [60]. The interaction detector reveals the interactive influence between different factors on the dependent variable [62], that is to say, the interactive effects of factors x_i and x_k may weaken, enhance, or independently affect the ESV. The q(x_i) and q(x_k) of driving factor x_i and x_k were obtained from the above factor detector. The symbol '∩' denotes the intersection between factors x_i and x_k [59]. The q-statistic value for the interaction between two factors on the ESV is written as (q (x_i ∩x_k)). Specific categories of interactions are given in Table S1 in the Supplementary Materials. The geodetector method was performed using the Geodetector package (https://cran.r-project.org/web/packages/geodetector/index.html (accessed on 20 May 2022) in R (v.4.2.1) software.

Additionally, it is worth noting that the problem of multicollinearity between factors may weaken the accuracy of the model predictions. Therefore, before using geographical detector analysis, it is crucial to analyze the multicollinearity of factors on the ESV. In many studies, the tolerance and variance inflation factor (VIF) have been commonly used methods for detecting multicollinearity. When tolerance was less than 0.1 or VIF greater than 10, it indicated severe multicollinearity and given some cause for concern [63,64]. Furthermore, the high VIF meant a significant multicollinearity between factors [65]. In this study, multicollinearity analysis was performed on the dominant factors (Table S2). The tolerance values of all factors were greater than 0.1, and the values of VIF were less than 10, indicating that all the factors are free from serious multicollinearity problems. However, the VIF value of FVC was less than 10, but very close to 10, so we deleted this factor.

3. Results

3.1. The Spatiotemporal Changes of the ESV

The patterns of the ESV presented an overall increasing trend from the northwest to the southeast portions of the study area (Figure 3). The Qilian Mountains were characterized by high the ESV, which were consistent with high vegetation cover and plenty of rainfall. The low-value areas of the ESV were mainly located in the Hexi Corridor, with strong evaporation, scarce water resources, and sparse vegetation. For example, in 2020, the ecosystem services value of the Qilian Mountains and the Hexi Corridor accounted for 92.29% and 7.71% of the entire study area (2667.72 $\times$ 10^8 CNY), respectively. In 2020 and 2050, the ESV was significantly higher than that in 1980 (Tables 2 and 3). Specifically, the ESV increased by 562.96 $\times$ 10^8 CNY from 1980 to 2020 (Table 2), with the Qilian Mountains and Hexi Corridor increasing by 536.95 $\times$ 10^8 CNY and 26.01 $\times$ 10^8 CNY, respectively. Additionally, the total ESV will increase by 91.57 $\times$ 10^8 CNY from 2020 to 2050 under the EP scenario, which is higher than that in the ND and RU scenarios. From 1980 to 2020, the increasing areas of ESV changes occurred in the oases and the east Qilian Mountains.

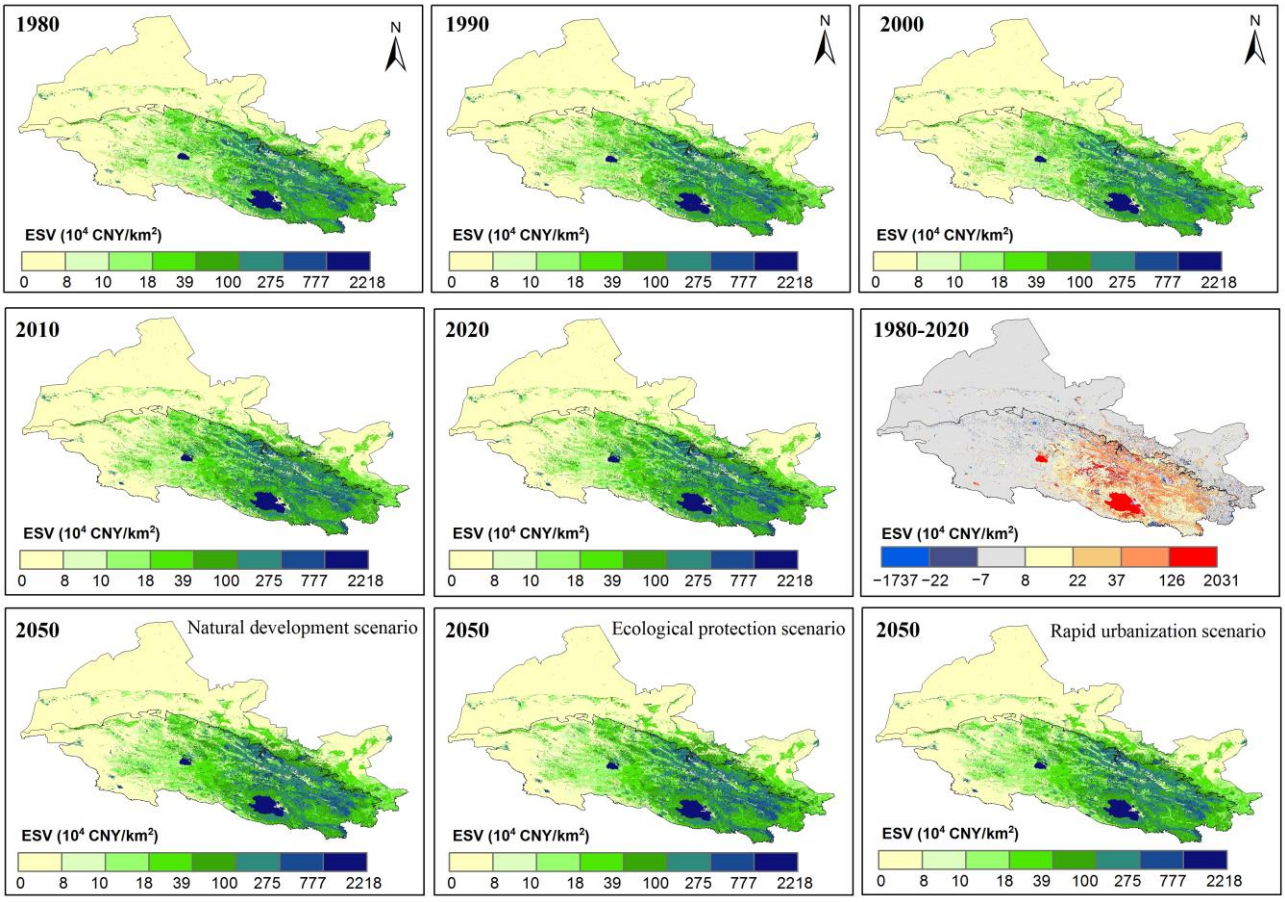

Figure 3. The spatial distribution of the ESV from 1980 to 2050 in the Hexi Regions, China.

Tables 2 and 3 show that the four sub-categories of ESV contributed diversely to the total ESV in the Hexi Regions. With an increasing trend in fluctuation from 1980 to 2020, the value of regulating services reached 1934.74 $\times$ 10^8 CNY in 2020, which accounted for 72.52% of the total ESV. The supporting services and provisioning services accounted for 15.60% and 8.49% of the total ESV in 2020, respectively. The ESV of the cultural service was minimal, accounting for only 3.38% of the total ESV. Climate regulation, hydrological regulation, soil conservation, and biodiversity were the four predominant ecosystem services in the Hexi Regions (Tables 2 and 3). In 2020, hydrological regulation and climate regulation accounted for 46.87 and 14.23% of the total ESV, respectively. The value of the other

ecosystem services was less than 10% of the total ESV, especially the values for food supply, raw material supply, and maintaining nutrient cycling. Over the past 40 years, water, high-cover grasslands, shrublands, forests, medium-cover grasslands, and swamplands in the Hexi Regions have contributed more than 80% to the ESV, and these areas continue to grow (Figure 4), increasing by approximately 259.03 $\times$ 10^8 CNY, 89.02 $\times$ 10^8 CNY, 42.78 $\times$ 10^8 CNY, 34.89 $\times$ 10^8 CNY, 33.20 $\times$ 10^8 CNY, and 45.56 $\times$$10^8$ CNY, respectively. As of 2020, the ESV changes in cropland in the Hexi Corridor under the EP scenario was much greater than that in the mountainous regions.

Table 2. The ESV in the Hexi Regions from 1980 to 2020 (Unit:10^8 CNY).

Ecosystem Services		1980			2020			Changes (1980–2020)		
Primary Types	**Secondary Types**	**HX**	**QM**	**Total**	**HX**	**QM**	**Total**	**HX**	**QM**	**Total**
Provisioning Services	Food supply	11.42	32.60	44.02	14.27	39.44	53.71	2.85	6.84	9.69
	Raw material supply	6.84	36.56	43.40	8.29	44.17	52.46	1.44	7.61	9.05
	Water supply	6.17	88.28	94.45	7.01	113.44	120.45	0.83	25.16	26.00
	Subtotal	24.44	157.44	181.87	29.56	197.05	226.62	5.13	39.62	44.74
Regulating Services	Gas regulation	14.90	115.20	130.09	17.63	139.59	157.22	2.73	24.39	27.12
	Climate regulation	22.52	292.35	314.88	25.28	354.46	379.74	2.76	62.10	64.86
	Environment purification	9.33	111.77	121.09	10.27	137.07	147.34	0.94	25.30	26.25
	Hydrological regulation	75.27	871.75	947.01	85.62	1164.82	1250.44	10.35	293.07	303.42
	Subtotal	122.02	1391.06	1513.08	138.80	1795.93	1934.74	16.79	404.87	421.66
Supporting Services	Soil conservation	15.04	154.04	169.08	17.10	197.48	214.58	2.06	43.44	45.50
	Maintaining nutrient cycling	2.07	11.71	13.78	2.51	14.16	16.67	0.44	2.45	2.89
	Biodiversity	10.80	141.80	152.61	11.89	173.00	184.89	1.09	31.19	32.28
	Subtotal	27.91	307.56	335.47	31.50	384.64	416.14	3.59	77.08	80.67
Cultural services	Aesthetic landscape	5.24	69.09	74.33	5.75	84.47	90.23	0.51	15.38	15.89
	Total	179.61	1925.15	2104.76	205.62	2462.10	2667.72	26.01	536.95	562.96

Note: HX, Hexi Corridor; QM, Qilian Mountains.

Table 3. The ESV in the Hexi Regions under different scenarios in 2050 (Unit: 10^8 CNY).

Ecosystem Services		2050 ND			2050 EP			2050 RU			Changes (2020–2050)		
Primary Type	**Secondary Types**	**HX**	**QM**	**Total**	**HX**	**QM**	**Total**	**HX**	**QM**	**Total**	**NG**	**EP**	**UD**
Provisioning Services	FS	16.53	37.75	54.28	17.82	39.37	57.19	15.43	35.64	51.07	0.56	3.48	−2.64
	RMS	9.34	43.24	52.58	10.11	45.21	55.32	8.71	40.40	49.11	0.12	2.86	−3.35
	WS	6.93	110.13	117.06	8.66	114.54	123.20	6.53	102.87	109.40	−3.38	2.76	−11.05
	Subtotal	32.81	191.12	223.92	36.59	199.12	235.71	30.68	178.91	209.58	−2.70	9.09	−17.04
Regulating Services	GR	19.26	137.87	157.12	20.92	143.93	164.86	17.89	128.51	146.39	−0.09	7.64	−10.82
	CR	25.61	352.07	377.67	28.17	368.41	396.57	23.53	327.03	350.56	−2.07	16.83	−29.19
	EP	10.53	136.03	146.57	11.84	141.54	153.39	9.84	126.64	136.48	−0.77	6.04	−10.86
	HR	84.98	1123.39	1208.37	106.39	1181.50	1287.89	80.13	1040.21	1120.34	−42.07	37.45	−130.10
	Subtotal	140.38	1749.35	1889.73	167.33	1835.38	2002.70	131.38	1622.38	1753.76	−45.00	67.97	−180.98
Supporting Services	SC	17.07	189.63	206.70	18.16	200.51	218.67	16.33	172.91	189.24	−7.88	4.08	−25.34
	MNC	2.81	13.89	16.70	3.04	14.51	17.55	2.62	12.98	15.60	0.03	0.88	−1.07
	BIO	12.03	171.78	183.80	13.26	178.23	191.48	11.13	159.65	170.78	−1.09	6.59	−14.12
	Subtotal	31.91	375.30	407.21	34.46	393.24	427.70	30.07	345.54	375.61	−8.94	11.56	−40.53
Cultural services	AL	5.82	83.81	89.63	6.43	86.75	93.18	5.39	77.93	83.33	−0.60	2.96	−6.90
	Total	210.91	2399.58	2610.49	244.81	2514.48	2759.29	197.52	2224.76	2422.28	−57.23	91.57	−245.45

Note: HX, Hexi Corridor; QM, Qilian Mountains; ND: natural development scenario; EP: ecological protection scenario; UR: rapid urbanization scenario. FS, food supply; RMS, raw material supply; WS, water supply; GR, gas regulation; CR, climate regulation; EP, environment purification; HR, hydrological regulation; SC, soil conservation; MNC, maintaining nutrient cycling; BIO, biodiversity; AL, aesthetic landscape.

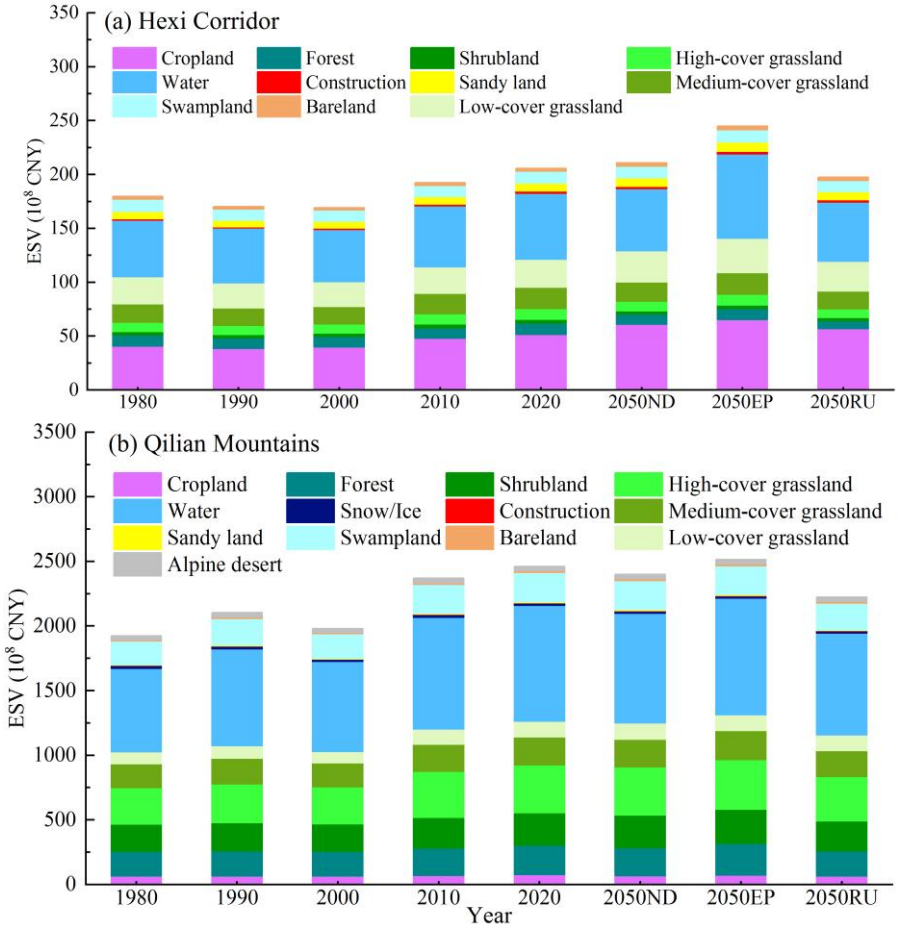

Figure 4. The ESV for different land use types in the Hexi Regions from 1980 to 2050. Note: ND: natural development scenario; EP: ecological protection scenario; RU: rapid urbanization scenario.

3.2. Trade-Offs and Synergies among Ecosystem Services Based on ESV

To reveal the steady trade-offs and synergies between ecosystem services based on the ESV, the positive and negative correlation was performed using four ecosystem services from 1980 to 2050. The results showed that all four ecosystem services in the Hexi Corridor had significant synergistic relationships with each other during the study periods (Figure 5a,c), and cultural services exhibits a strong synergistic relationship with supporting services, and provisioning services are positively correlated with regulating services; the interaction among these ecosystem services was obvious because of the high correlation coefficient, i.e., there were strong synergies between ecosystem services. In the Qilian Mountains, the relationships between ecosystem services were also dominated by strong synergistic relationships (Figure 5b,d). Among these, there were strong synergistic relationships between cultural, provisioning, regulating, and supporting services, which were similar to those of the Hexi Corridor. Moreover, provisioning services also had a stronger synergistic relationship with regulating services than that noted in the mountains. The synergistic relationship of cultural services and regulating services in the Qilian Mountains was slightly less than that of Hexi Corridor. In addition, there were slightly weak synergies between supporting services, provisioning services, and regulating services, compared to those in the Hexi Corridor. In short, from the past to the future, the correlation coefficient between ecosystem services fluctuated slightly in the Hexi Regions, but was generally stable and characterized by synergistic relationships.

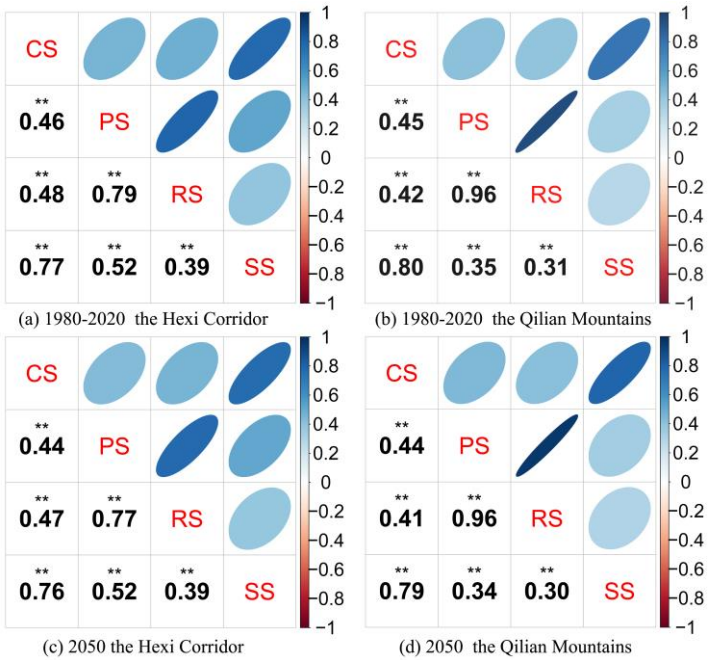

Figure 5. Pearson correlations between pairs of ecosystem services based on ESV in the Hexi Regions, China, from 1980 to 2050. Note: PS: provisioning services; RS: regulating services; SS: supporting services; CS: cultural services. The blue and red colors indicate positive and negative correlations, respectively. Meanwhile, the number is the Pearson correlation coefficient. ** represents that the correlations are significant at the 0.01 level.

As shown in Figure 6, spatially, the relationships of four ecosystem services based on ESV in the study periods were mainly dominated by synergistic relationships between the high-high cluster and the low-low cluster in the Hexi Regions, with significant spatial heterogeneity. Furthermore, the synergistic relationship between the high-high cluster and ecosystem services (i.e., provisioning services with supporting services, cultural services) was largely concentrated in the southeast Qilian Mountains, an area with abundant water resources and high vegetation coverage. Therefore, provisioning services and cultural services benefited, to a certain extent, from regulating services and supporting services in this region. For instance, higher provisioning services were associated with higher supporting services in the Qilian Mountains, approximately 26.86% of the whole study area during 1980 to 2020. Compared with the Qilian Mountains, the Hexi Corridor, experiencing drought and water shortage, exhibited a low-low agglomeration of synergistic relationships among ecosystem services. For example, the distribution of lower regulating services was more consistent with lower supporting services in the low altitudes of arid regions, and this synergistic relationship of low-low aggregation accounted for approximately 35.50% of the Hexi Regions over the past 40 years. Additionally, the trade-off relationships among ecosystem services in the whole Hexi Regions were relatively weak (Figure 6). In the Qilian Mountains, the trade-offs were primarily distributed in the glacial region of the western mountains, with a high proportion of high-low trade-offs for provisioning services and supporting services. In other words, abundant water sources, higher elevation, and lower vegetation coverage in this region have resulted in lower supporting services (i.e., soil conservation and biodiversity) in these areas. Compared with 2020, in 2050, the relationships among ecosystem services in the entire study area generally decreased in synergies and increased in trade-offs.

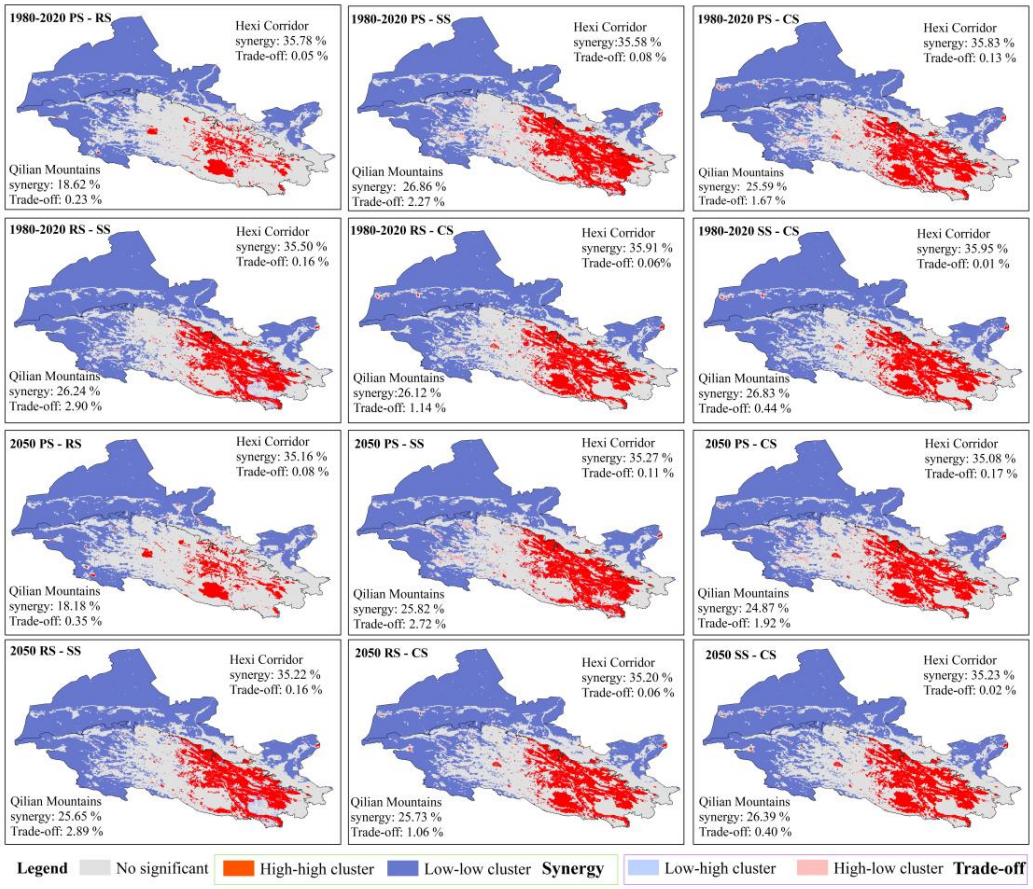

Figure 6. LISA cluster map of ecosystem services based on ESV in the Hexi Regions from 1980 to 2050. PS: provisioning services; RS: regulating services; SS: supporting services; CS: cultural services. High-high and low-low clusters indicate synergistic relationships, and high-low and low-high clusters indicate trade-off relationships. The numbers indicate trade-offs and synergies as a percentage of the overall study area.

3.3. Drivers of Ecosystem Services Value

We analyzed the role of each driver in altering the spatial heterogeneity of the ESV (Table 4). The results suggested that the spatial heterogeneity of the ESV in the Hexi Regions was affected by a combination of socioeconomic and natural factors. In the Hexi Corridor, the q value of LUCC was 0.35, accounting for more than 35.39% of variation in the spatial differentiation of the ESV over the last 40 years; the annual mean precipitation, NPP, and potential evapotranspiration explained more than 5% of the spatial differentiation of the ESV. Although the explanatory power of other factors was less than 5%, especially regarding socioeconomic factors, they also played a crucial role in the ESV. Compared with the Hexi Corridor, the LUCC with the highest q value (0.80) predominantly explained 80.06% of the ESV in the Qilian Mountains from 1980 to 2020, followed by potential evapotranspiration (15.28%), annual mean precipitation (14.27%), soil organic carbon density (11.99%), annual average temperature (9.37%), elevation (6.57%), and NPP (5.54%). Furthermore, in the mountains, human factors, such as GDP, population, road density, and distance to the settlement, had a weaker explanatory influence on the ESV. This implies that LUCC, climate, and vegetation were important for the ESV in the Qilian Mountains over the long term. From 1980 to 2050, the q values of LUCC and GDP slightly increased in the Hexi Regions. The q values of the annual mean precipitation, annual mean temperature, NPP, elevation, etc., were lightly reduced in these regions. However, LUCC, climate and vegetation have still been important factors affecting the ESV of the entire Hexi Regions over the study periods, which provides a basis for the scientific assessment of the ESV.

Table 4. The factors affecting the ESV in the Hexi Regions from 1980 to 2050.

Factors	1980-2020				2050			
	Hexi Corridor		Qilian Mountains		Hexi Corridor		Qilian Mountains	
	q-Value	*p*-Value	q-Value	*p*-Value	q-Value	*p*-Value	q-Value	*p*-Value
DEM	0.019	0.000	0.066	0.000	0.013	0.000	0.064	0.000
SUR	0.007	0.000	0.002	0.000	0.006	0.000	0.002	0.000
SLE	0.009	0.000	0.043	0.000	0.006	0.000	0.045	0.000
PRE	0.108	0.000	0.143	0.000	0.084	0.000	0.117	0.000
TMP	0.005	0.000	0.094	0.000	0.004	0.000	0.091	0.000
PET	0.072	0.000	0.153	0.000	0.059	0.000	0.155	0.000
NPP	0.085	0.000	0.055	0.000	0.076	0.000	0.053	0.000
LUC	0.354	0.000	0.801	0.000	0.557	0.000	0.835	0.000
SOC	0.046	0.000	0.120	0.000	0.034	0.000	0.123	0.000
GDP	0.024	0.000	0.001	0.000	0.038	0.000	0.019	0.000
POP	0.034	0.000	0.000	0.000	0.010	0.000	0.000	0.000
DTS	0.033	0.000	0.004	0.000	0.034	0.000	0.004	0.000
ROD	0.014	0.000	0.019	0.000	0.014	0.000	0.019	0.000

Note: The *p* values were all tested for 5% significance. DEM, elevation; SUR, surface roughness; SLE, slope; PRE, annual mean precipitation; TMP, annual mean temperature; PET, potential evapotranspiration; NPP, net primary productivity; LUC, land use and land cover change; SOC, soil organic carbon density; GDP, gross domestic product; POP, population; DTS: distance to settlement; ROD, road density.

The interactive effects of environmental factors on the ESV from 1980 to 2050 are shown in Figure 7. The explanatory power ($q(x_i \cap x_k)$) of any two drivers over the ESV was strengthened after their interaction effect, either bilaterally or nonlinearly, indicating that the interaction can exert larger impacts on the ESV than each one on its own. Therefore, the combined effects of these driving factors on the ESV were mutually promoting. Specifically, the interactive effects of factors such as GDP, POP, distance to settlement, road density, LUCC, and NPP on ESV in the Hexi Corridor have been mutually enhanced (Figure 7a,c), but this enhancement was not strong. For example, the q values of LUCC and NPP were 0.35 and 0.08, respectively (Figure 7a), and the q value of their interaction reached 0.40 ($Max(q(LUC), q(NPP)) < q(LUC \cap NPP) < q(LUC) + q(NPP)$. The q values of LUCC and PET were 0.35 and 0.07, respectively (Figure 7a), and the q value of their interaction reached 0.44. Furthermore, among the pairs of natural factors, the dominant interactive power q value was LUCC that interacted with elevation, slope, precipitation, temperature and potential evapotranspiration in the Hexi Corridor. Their q values were 0.42, 0.38, 0.47, 0.42 and 0.44, respectively. This indicated that that the interaction between climate and LUCC exerted larger impacts on ESV than did the other socioeconomic factors.

Similar results were obtained in the Qilian Mountains. The dominant power of the natural factors was stronger than that of the anthropogenic factors, suggesting that natural factors significantly contributed to high ESV. However, the interactive effects of environmental factors on ESV in the Qilian Mountains were mostly nonlinearly enhanced with higher q value (the red number in Figure 7b,d), except that the effects of LUCC and terrain, climate, vegetation, soil, and other factors were bilaterally enhanced. In addition, the interaction of human activities and natural conditions exhibits enhanced effects on ESV in mountainous areas. For instance, the q value of road density (ROD) was 0.02, and the q value of NPP was 0.06 over the past 40 years. The q value reached 0.12 ($q(ROD \cap NPP) > q(ROD) + q(NPP)$) after their interaction. The q value of distance to settlement (DTS) was 0.004, and the q value of potential evapotranspiration (PET) was 0.153 for the past 40 years. The q value reached 0.21 ($q(DTS \cap PET) > q(DTS) + q(PET)$) after their interaction. The interactive effects of LUCC and natural factors were stronger than those for other natural factors during 1980 to 2050. For example, the interaction of LUCC and precipitation can explain nearly 88% of the ESV. The dominant interaction effect on ESV was LUCC interacting with population density, GDP, and the distance to the settlement, with the higher q values of 0.80, 0.80, and 0.81, respectively. Furthermore, natural factors

such as topography and climate tended to amplify the influence of human activities in the mountains.

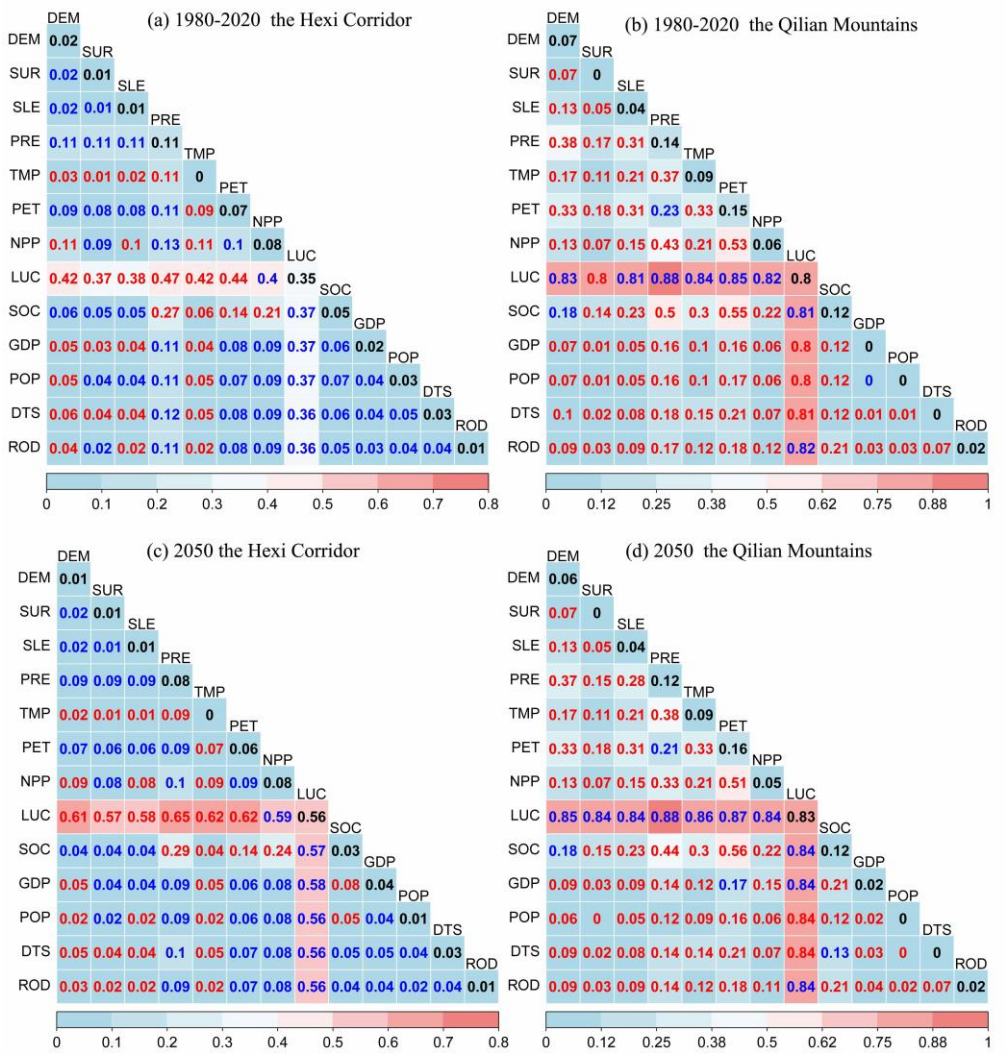

Figure 7. Interactive effects of each factor pair on the ESV in the Hexi Regions from 1980 to 2050. Note: Numbers in the black, red and blue squares indicate q values. The black numbers indicate the effect of two same factors on ESV. The red and blue colors of the numbers represent the type of interaction between the two factor as non-linearly enhanced and bilaterally enhanced, respectively. DEM, elevation; SUR, surface roughness; SLE, slope; PRE, annual mean precipitation; TMP, annual mean temperature; PET, potential evapotranspiration; NPP, net primary productivity; LUC, land use and land cover change; SOC, soil organic carbon density; GDP, gross domestic product; POP, population; DTS: distance to settlement; ROD, road density.

4. Discussion

4.1. Changes in the ESV in Different Regions

Our results demonstrated that the ESV in the mountains was much higher than in the plains, and similar results were also found in previous studies [37,66]. For example, the value of ecosystem services in the lower, middle, and upper reaches of the Lhasa River were 74.35%, 21.48%, and 4.17%, respectively, which showed significant spatial heterogeneity of ESV [67]. The ESV of the Hexi Regions has increased significantly, with the Qilian Mountains and Hexi Corridor increasing by 536.95 $\times$ 10^8 CNY and 26.01 $\times$ 10^8 CNY, respectively, over the past four decades. The results were similar to those for the arid inland regions, such as central Asia. For example, related results showed an increase of USD 87 billion in the ESV between 1950 and 2000 in Pakistan due to the construction of dams

and the subsequent agricultural expansion into the deserts [68]. As result of environmental changes or spatiotemporal scales, the effects on the ESV have fluctuated, rather than linearly decreasing or increasing. Qian et al. [69] found that the regional ESV decreased as mining areas expanded, accelerating with the loss of the ESV of wetlands and hydrological regulation function in the of Qilian Mountains. Meanwhile, the value of regulating services showed an increasing trend in the Hexi Regions over the past 40 years, decreasing in the 2050 for the RU and ND scenarios compared to 2020. Moreover, in 2050, under the EP scenario, the increase in the total ESV in Qilian Mountains was attributed to the increase in forests, shrublands, grasslands, and water areas. Previous studies showed that the total ESV under the ecological protection scenario was higher than that in the natural increase scenario and economic development scenario in the Wuhan urban agglomeration, China [70]. In this study, the water, high-cover grassland, shrubland, forest, medium-cover grassland, and swampland have contributed to exceeded 80% of the total ESV, and similar results were also presented in other studies [71]. The increase in total ESV of the Hexi Corridor during 1980–2020 was mainly associated with the conversion of low-cover grassland and sandy land to cropland (Figures 4 and S2); the improved grassland and increase in water were the main reasons for the increase in total ESV in the Qilian Mountains (Figures 4 and S3). Recent studies have also found that the increase in forests and water bodies was conducive to the enhancement of the total ESV in the Yiluo River Basin, which was a significant tributary in the Yellow River of China during 2000 to 2020 [29]. In addition, compared to 2020, the expansion of construction land and cropland in the Hexi Corridor led to a decline of the total ESV in 2050 under the rapid urbanization scenario. This pattern has also been found in other studies of oases in arid regions. For example, farmland expansion in the Shule River Basin in northwest China occurred at the expense of high-ESV lands such as woodlands, grasslands, wetlands, and water bodies [41].

4.2. The Synergies and Trade-Offs Relationships of Ecosystem Services

Our results showed that relationships between each of the four ecosystem services in the study periods were dominated by strong synergies and weak trade-offs, with significant spatial heterogeneity in the Hexi Regions (Figures 5 and 6). These results are consistent with the findings of previous studies in other regions [72,73]. For example, the relationships among supply services and regulation services in the Poyang Lake Basin, as the largest freshwater lake in China, were mainly synergies, with few trade-offs due to the vast water surface, high water supply capacity, and the dense vegetation of the wetlands [74]. Furthermore, the synergistic relationships of the high-high cluster and ecosystem services were largely concentrated in the southeast of the Qilian Mountains; the Hexi Corridor exhibited a low-low cluster of synergistic relationships among ecosystem services due to drought and water shortage; the trade-offs mainly occurred over the glaciers regions of the western Qilian Mountains, with the high-low trade-offs for provisioning services and supporting services. Mountain glaciers performed the irreplaceable ecological services, such as climate regulation and freshwater resource supply, in the arid inland regions, while its biodiversity/habitat function was significantly lower than that of other land cover types [75]. Many studies have examined the spatial differences of these relationships among ecosystem services at different scales due to complex environment background. For example, Pan et al. [76] found that there was a trade-off between food provision and soil conservation in the arid inland regions of northwestern China. Hulvey et al. [77] showed that livestock production and water quality had a trade-off in the semi-arid rangelands of northeastern Utah, USA, due to unreasonable grazing. Meanwhile, related studies have also given attention to the interactions among ecosystem services in different scenarios analyses. For instance, in the Tianshan Mountains of China, the trade-off effect in the Yili River Valley was obviously weakened between carbon storage and nutrient export under the ecological conservation scenario compared to that under the business as usual and economic development scenario [78].

4.3. Drivers of the ESV

The results demonstrated that the spatial heterogeneity of the ESV in the Hexi Regions was determined by the combined effects of socioeconomic and natural factors (Figure 7), which was consistent with the results of existing studies on the drivers of ESV [41]. Meanwhile, LUCC was the dominant driver for a long-time series of the ESV, followed by climate and vegetation, significantly affecting the ESV in the Hexi Regions over the long term. Previous research conducted in the China-Mongolia-Russia Economic Corridor indicated that LUCC could exert significant impacts on the ESV, and land-use category conversion, such as desertification, farmland expansion, and urbanization, negatively affect the ESV, while the conversion of farmland and bare lands to forests and grasslands could positively affect the ESV [79]. Furthermore, compared with the Hexi Corridor, in mountains, human factors, such as GDP, population, and road density, exerted less impact on the ESV. Over the past 40 years, the ESV of cropland in the Hexi Corridor has significantly increased, and this was mainly associated with oasis expansion as a result of population growth. Researchers have pointed out that the population and cities were mainly concentrated in the oases of the Hexi Corridor, with a typical temperate desert climate, and that population growth and sufficient irrigation were the main driving forces of oasis expansion [80]. It should be noted that humans can achieve the maximum possible benefits by reasonable ecosystem restoration in the regions of long-term degraded ecosystem services [81]. Wen et al. [82] emphasized that adaptable intercropping improved multiple ecosystem services (e.g., water regulation, soil retention) by altering soil water allocation and balancing soil water. Natural factors significantly contributed to high ESV in the Hexi Regions compared to human factors, especially in the mountains. Specifically, the interactions of natural factors, such as altitude, temperature, precipitation, LUCC, vegetation, and soil, had greater effects on ESV than anthropogenic factors in the Qilian Mountains. For example, in the Qinghai–Tibet Plateau, the ESV decreased with increasing elevation [83]. Moreover, natural factors tended to amplify the impact of human activities on ESV, especially in the Qilian Mountains. Similar results have been observed. Han et al. [21] found that natural factors (e.g., terrain, precipitation, temperature) significantly affected the spatial difference of the ESV in the hinterland of the Loess Plateau.

4.4. Management Implication and Limitation

Our results have demonstrated that there were obvious spatial differences in ecosystem services value, relationships, and driving factors in the Hexi Regions. Meanwhile, the total ESV under the EP scenario was estimated to experience an increase by 2050, which is estimated to be higher than the increase under the RU and ND scenarios. Forests, grasslands, swamplands, and water should be reasonably protected and conserved in order to maintain and enhance total ESV in the Hexi Regions. In the Hexi Corridor, with an arid climate and limited water resources, the expansion of croplands under climate change and intense human activities were conducive to an increase in ESV in a short time period. However, croplands expanded and urbanization intensified water consumption in the arid regions, threatening regulating and supporting services in the long run [84]. The governments and local authorities ought to develop sustainable agriculture and water-saving irrigation systems, balancing ecological and agricultural water use, which will achieve food security, water security, and ecological security. Additionally, the grassland improved and water increased in a warm and humid climate, and vegetation restoration contributed to an increase in ESV in the Qilian Mountains, with rich natural resources and more national nature reserves. In the face of complex climate change and human disturbance, there are still many challenges regarding ecological protection and restoration in the Qilian Mountains. For example, the mining activities in the southern parts of the Qilian Mountains have caused significant ESV loss in regards to meadows and wetlands [69]. Grasslands have been one of the main land types in the Qilian Mountains, and rotational grazing by reducing grazing duration and shifting its timing have mitigated ecosystem service trade-offs between vegetation productivity and other ecosystem regulating functions [77].

This study emphasized the effects of multiple factor interactions on ESV and identified ESV under multiple scenarios in complex ecosystems combined with human influence. The revised equivalent factor method, based on land cover data and socioeconomic data, has been widely applied to estimate ESV in China due to the advantages of reliability and operability [16,71,85]. It is convenient to facilitate comparisons with other existing research results. However, the ESV evaluation still exhibits some uncertainties due to intensified climate change and social development. For instance, it is difficult for us to quantify long-term economic value due to market prices and inflation [21]. The different land management policies of various decision makers also influences our cognitive level in the proposed scenarios of LUCC. In addition, the complexity and heterogeneity of natural–human systems caused the generalization of ESV in this method due to data quality and time span. In future work, we need to employ more detailed and long-term spatial datasets for improving ESV assessment and model establishment. Moreover, future research should consider additional climate model and human activity scenarios to reduce the impact of uncertainty on the simulation.

5. Conclusions

Our results showed that the ESV of the Qilian Mountains was about 10.27–11.97-fold greater than that of the Hexi Corridor. The ESV showed a significant increase from 1980 to 2050 for each of the three LUCC scenarios. Specifically, in the past 40 years, the ESV in the Hexi Regions has increased by 562.96×10^8 CNY, with the Qilian Mountains and Hexi Corridor increasing by 536.95×10^8 CNY and 26.01×10^8 CNY, respectively. The total ESV increased by 91.57×10^8 CNY from 2020 to 2050 under the EP scenario, which was higher than that in the ND and RU scenarios. Regulating services have contributed to exceed 70% of the total ESV, and decreased in the 2050 RU and ND scenarios compared with those for 2020. Moreover, in 2050, under the EP scenario, the increase in the total ESV in the Qilian Mountains was attributed to the increase in forests, shrublands, grasslands, and water. Our results also showed that relationships among ecosystem services were dominated by strong synergies and weak trade-offs, with significant spatial heterogeneity in the Hexi Regions. The spatial heterogeneity of the ESV in the Hexi Regions was determined by a combined effect of socioeconomic and natural factors. LUCC was the dominant driver, followed by climate and vegetation, significantly affecting the ESV in the Hexi Regions in the long term. Specifically, in the last 40 years, LUCC explained 35.39% and 80.06% of the ESV variation in the Hexi Corridor and the Qilian Mountains, respectively. The natural factors played a more important role in ESV changes than did the anthropogenic factors. The interaction of human activities and natural conditions has enhanced effects on ESV in mountainous areas. Our results highlighted the fundamental role of ecological protection and climate change in improving the ESV and managing ecosystem services for arid inland regions. Additionally, our research highlighted that a comprehensive analysis of ESV changes and driving mechanisms under different future scenarios based on LUCC simulation and geographical detector is necessary to realize more sustainable ecosystem services in future development, providing a reference for policy decisions in land management, ecological compensation, and the construction of ecological security patterns between the mountainous and plain regions in other arid inland regions.

Supplementary Materials: The following supporting information can be downloaded at: https://www.mdpi.com/article/10.3390/su142114164/s1, Figure S1: The spatial distribution of LUCC from 1980 to 2050 in the Hexi Regions, China; Figure S2: Chord diagrams of land use and land cover conversion during 1980–2050 in the Hexi Corridor; Figure S3: Chord diagrams of land use and land cover conversion during 1980–2050 in Qilian Mountains; Table S1: Types of interaction between two covariates; Table S2: Multicollinearity analysis of influencing factors on the ESV.

Author Contributions: Conceptualization, Y.L, W.L. and Q.F.; methodology, Y.L., M.Z. and L.Y.; software, Y.L, M.Z. and J.Z.; resources, Q.F., M.Z., J.Z. and X.Y.; writing—original draft preparation, Y.L.; writing—review and editing, Y.L., W.L. and M.Z.; funding acquisition, W.L. All authors have read and agreed to the published version of the manuscript.

Funding: This work was supported by the National Key R&D Program of China (No. 2022YFF1303301), the Key R&D Program of Gansu Province, China (Grant No. 20YF8FA002), the National Natural Science Fund of China (Grant No. 52179026, 42001035, 42101115), the Strategic Research and Consulting Project of the Chinese Academy of Engineering (2022-XY-24), the Science and Technology Project of Gansu Province (Grant No. 21ZD4NF044-02), and the Forestry and Grassland Science and Technology Innovation Program of Gansu Province (Grant No. GYCX [2020]01).

Institutional Review Board Statement: Not applicable.

Informed Consent Statement: Not applicable.

Data Availability Statement: Not applicable.

Acknowledgments: We would like to thank the team of Jiang Tong from the Institute for Disaster Risk Management, Nanjing University of Information Science & Technology, Nanjing Jiangsu, China. The team provided us with gridded datasets for the population and the economy under Shared Socioeconomic Pathways.

Conflicts of Interest: The authors declare no conflict of interest.

References

1. Costanza, R.; D'Arge, R.; de Groot, R.; Farber, S.; Grasso, M.; Hannon, B.; Limburg, K.; Naeem, S.; O'Neill, R.V.; Paruelo, J.; et al. The value of the world' s ecosystem services and natural capital. *Nature* **1997**, *387*, 253–260. [CrossRef]
2. Millennium Ecosystem Assessment, M.E.A. *Ecosystems and Human Well-Being*; Island Press: Washington, DC, USA, 2005.
3. Daw, T.; Brown, K.; Rosendo, S.; Pomeroy, R. Applying the ecosystem services concept to poverty alleviation: The need to disaggregate human well-being. *Environ. Conserv.* **2011**, *38*, 370–379. [CrossRef]
4. Sannigrahi, S.; Chakraborti, S.; Joshi, P.K.; Keesstra, S.; Sen, S.; Paul, S.K.; Kreuter, U.; Sutton, P.C.; Jha, S.; Dang, K.B. Ecosystem service value assessment of a natural reserve region for strengthening protection and conservation. *J. Environ. Manag.* **2019**, *244*, 208–227. [CrossRef] [PubMed]
5. Laurans, Y.; Rankovic, A.; Bille, R.; Pirard, R.; Mermet, L. Use of ecosystem services economic valuation for decision making: Questioning a literature blindspot. *J. Environ. Manag.* **2013**, *119*, 208–219. [CrossRef]
6. Xie, G.; Zhang, C.; Zhen, L.; Zhang, L. Dynamic changes in the value of China's ecosystem services. *Ecosyst. Serv.* **2017**, *26*, 146–154. [CrossRef]
7. Naselli-Flores, L.; Padisák, J. Ecosystem services provided by marine and freshwater phytoplankton. *Hydrobiologia* **2022**. [CrossRef] [PubMed]
8. Costanza, R.; de Groot, R.; Sutton, P.; van der Ploeg, S.; Anderson, S.J.; Kubiszewski, I.; Farber, S.; Turner, R.K. Changes in the global value of ecosystem services. *Glob. Environ. Chang.* **2014**, *26*, 152–158. [CrossRef]
9. Díaz, S.; Settele, J.; Brondízio, E.S.; Ngo, H.T.; Agard, J.; Arneth, A.; Balvanera, P.; Brauman, K.A.; Butchart, S.H.M.; Chan, K.M.A.; et al. Pervasive human-driven decline of life on Earth points to the need for transformative change. *Science* **2019**, *366*, x3100. [CrossRef]
10. Xiao, Y.; Huang, M.; Xie, G.; Zhen, L. Evaluating the impacts of land use change on ecosystem service values under multiple scenarios in the Hunshandake region of China. *Sci. Total Environ.* **2022**, *850*, 158067. [CrossRef]
11. He, X.; Liang, J.; Zeng, G.; Yuan, Y.; Li, X. The Effects of Interaction between Climate Change and Land-Use/Cover Change on Biodiversity-Related Ecosystem Services. *Glob. Chall.* **2019**, *3*, 1800095. [CrossRef]
12. Zhang, L.; Lü, Y.; Fu, B.; Zeng, Y. Uncertainties of Two Methods in Selecting Priority Areas for Protecting Soil Conservation Service at Regional Scale. *Sustainability* **2017**, *9*, 1577. [CrossRef]
13. Berihun, M.L.; Tsunekawa, A.; Haregeweyn, N.; Meshesha, D.T.; Adgo, E.; Tsubo, M.; Masunaga, T.; Fenta, A.A.; Sultan, D.; Yibeltal, M. Exploring land use/land cover changes, drivers and their implications in contrasting agro-ecological environments of Ethiopia. *Land Use Policy* **2019**, *87*, 104052. [CrossRef]
14. Schirpke, U.; Kohler, M.; Leitinger, G.; Fontana, V.; Tasser, E.; Tappeiner, U. Future impacts of changing land-use and climate on ecosystem services of mountain grassland and their resilience. *Ecosyst. Serv.* **2019**, *26*, 79–94. [CrossRef] [PubMed]
15. Allan, E.; Manning, P.; Alt, F.; Binkenstein, J.; Blaser, S.; Blüthgen, N.; Böhm, S.; Grassein, F.; Hölzel, N.; Klaus, V.H.; et al. Land use intensification alters ecosystem multifunctionality via loss of biodiversity and changes to functional composition. *Ecol. Lett.* **2015**, *18*, 834–843. [CrossRef] [PubMed]

16. Li, W.; Wang, L.; Yang, X.; Liang, T.; Zhang, Q.; Liao, X.; White, J.R.; Rinklebe, J. Interactive influences of meteorological and socioeconomic factors on ecosystem service values in a river basin with different geomorphic features. *Sci. Total Environ.* **2022**, *829*, 154595. [CrossRef] [PubMed]
17. Su, K.; Wei, D.; Lin, W. Evaluation of ecosystem services value and its implications for policy making in China – A case study of Fujian province. *Ecol. Indic.* **2020**, *108*, 105752. [CrossRef]
18. Ouyang, Z.; Song, C.; Zheng, H.; Polasky, S.; Xiao, Y.; Bateman, I.J.; Liu, J.; Ruckelshaus, M.; Shi, F.; Xiao, Y.; et al. Using gross ecosystem product (GEP) to value nature in decision making. *Proc. Natl. Acad. Sci. USA* **2020**, *117*, 14593–14601. [CrossRef]
19. Boumans, R.; Roman, J.; Altman, I.; Kaufman, L. The Multiscale Integrated Model of Ecosystem Services (MIMES): Simulating the interactions of coupled human and natural systems. *Ecosyst. Serv.* **2015**, *12*, 30–41. [CrossRef]
20. Xie, G.; Zhen, L.; Lu, C.; Xiao, Y.; Chen, C. Expert Knowledge Based Valuation Method of Ecosystem Services in China. *J. Nat. Resour.* **2008**, *23*, 911–919.
21. Han, X.; Yu, J.; Shi, L.; Zhao, X.; Wang, J. Spatiotemporal evolution of ecosystem service values in an area dominated by vegetation restoration: Quantification and mechanisms. *Ecol. Indic.* **2021**, *131*, 108191. [CrossRef]
22. Bagstad, K.J.; Semmens, D.J.; Waage, S.; Winthrop, R. A comparative assessment of decision-support tools for ecosystem services quantification and valuation. *Ecosyst. Serv.* **2013**, *5*, 27–39. [CrossRef]
23. Kusi, K.K.; Khattabi, A.; Mhammdi, N.; Lahssini, S. Prospective evaluation of the impact of land use change on ecosystem services in the Ourika watershed, Morocco. *Land Use Policy* **2020**, *97*, 104796. [CrossRef]
24. Song, W.; Deng, X. Land-use/land-cover change and ecosystem service provision in China. *Sci. Total Environ.* **2017**, *576*, 705–719. [CrossRef]
25. de Oliveira Barros, K.; Alvares Soares Ribeiro, C.A.; Marcatti, G.E.; Lorenzon, A.S.; Martins De Castro, N.L.; Domingues, G.F.; Romário De Carvalho, J.; Rosa Dos Santos, A. Markov chains and cellular automata to predict environments subject to desertification. *J. Environ. Manag.* **2018**, *225*, 160–167. [CrossRef] [PubMed]
26. Gao, X.; Wang, J.; Li, C.; Shen, W.; Song, Z.; Nie, C.; Zhang, X. Land use change simulation and spatial analysis of ecosystem service value in Shijiazhuang under multi-scenarios. *Environ. Sci. Pollut. Res. Int.* **2021**, *28*, 31043–31058. [CrossRef]
27. Lang, Y.; Song, W. Quantifying and mapping the responses of selected ecosystem services to projected land use changes. *Ecol. Indic.* **2019**, *102*, 186–198. [CrossRef]
28. Li, X.; Chen, Y.; Liu, X.; Li, D.; He, J. Concepts, methodologies, and tools of an integrated geographical simulation and optimization system. *Int. J. Geogr. Inf. Sci.* **2011**, *25*, 633–655. [CrossRef]
29. Hou, J.; Qin, T.; Liu, S.; Wang, J.; Dong, B.; Yan, S.; Nie, H. Analysis and Prediction of Ecosystem Service Values Based on Land Use/Cover Change in the Yiluo River Basin. *Sustainability* **2021**, *13*, 6432. [CrossRef]
30. Liang, X.; Guan, Q.; Clarke, K.C.; Chen, G.; Guo, S.; Yao, Y. Mixed-cell cellular automata: A new approach for simulating the spatio-temporal dynamics of mixed land use structures. *Landsc. Urban Plan* **2021**, *205*, 103960. [CrossRef]
31. Li, C.; Wu, Y.; Gao, B.; Zheng, K.; Wu, Y.; Li, C. Multi-scenario simulation of ecosystem service value for optimization of land use in the Sichuan-Yunnan ecological barrier, China. *Ecol. Indic.* **2021**, *132*, 108328. [CrossRef]
32. Liang, X.; Guan, Q.F.; Clarke, K.C.; Liu, S.S.; Wang, B.Y.; Yao, Y. Understanding the drivers of sustainable land expansion using a patch-generating land use simulation (PLUS) model: A case study in Wuhan, China. *Comput. Environ. Urban. Syst.* **2021**, *85*, 101569. [CrossRef]
33. Bennett, E.M.; Peterson, G.D.; Gordon, L.J. Understanding relationships among multiple ecosystem services. *Ecol. Lett.* **2009**, *12*, 1394–1404. [CrossRef] [PubMed]
34. Chen, T.; Peng, L.; Wang, Q. Response and multiscenario simulation of trade-offs/synergies among ecosystem services to the Grain to Green Program: A case study of the Chengdu-Chongqing urban agglomeration, China. *Environ. Sci. Pollut. Res.* **2022**, *29*, 33572–33586. [CrossRef] [PubMed]
35. Dade, M.C.; Mitchell, M.G.E.; McAlpine, C.A.; Rhodes, J.R. Assessing ecosystem service trade-offs and synergies: The need for a more mechanistic approach. *Ambio* **2019**, *48*, 1116–1128. [CrossRef]
36. Zheng, D.; Wang, Y.; Hao, S.; Xu, W.; Lv, L.; Yu, S. Spatial-temporal variation and tradeoffs/synergies analysis on multiple ecosystem services: A case study in the Three-River Headwaters region of China. *Ecol. Indic.* **2020**, *116*, 106494. [CrossRef]
37. Li, Y.; Liu, W.; Feng, Q.; Zhu, M.; Yang, L.; Zhang, J. Quantitative Assessment for the Spatiotemporal Changes of Ecosystem Services, Tradeoff–Synergy Relationships and Drivers in the Semi-Arid Regions of China. *Remote Sens.* **2022**, *14*, 239. [CrossRef]
38. Yao, J.; Liu, H.; Huang, J.; Gao, Z.; Wang, G.; Li, D.; Yu, H.; Chen, X. Accelerated dryland expansion regulates future variability in dryland gross primary production. *Nat. Commun.* **2020**, *11*, 1665. [CrossRef]
39. Qian, D.; Yan, C.; Xing, Z.; Xiu, L. Monitoring coal mine changes and their impact on landscape patterns in an alpine region: A case study of the Muli coal mine in the Qinghai-Tibet Plateau. *Environ. Monit. Assess.* **2017**, *189*, 513–559. [CrossRef]
40. Zhou, Z.; Han, N.; Liu, J.; Yan, Z.; Xu, C.; Cai, J.; Shang, Y.; Zhu, J. Glacier variations and their response to climate change in an arid inland river basin of Northwest China. *J. Arid Land.* **2020**, *12*, 357–373. [CrossRef]
41. Pan, N.; Guan, Q.; Wang, Q.; Sun, Y.; Li, H.; Ma, Y. Spatial Differentiation and Driving Mechanisms in Ecosystem Service Value of Arid Region: A case study in the middle and lower reaches of Shule River Basin, NW China. *J. Clean. Prod.* **2021**, *319*, 128718. [CrossRef]
42. Feng, Q.; Yang, L.S.; Deo, R.C.; AghaKouchak, A.; Adamowski, J.F.; Stone, R.; Yin, Z.L.; Liu, W.; Si, J.H.; Wen, X.H.; et al. Domino effect of climate change over two millennia in ancient China's Hexi Corridor. *Nat. Sustain.* **2019**, *2*, 957–961. [CrossRef]

43. He, J.; Wang, N.; Chen, A.A.; Yang, X.; Hua, T. Glacier Changes in the Qilian Mountains, Northwest China, between the 1960s and 2015. *Water* **2019**, *11*, 623. [CrossRef]
44. Li, Y.; Liu, W.; Feng, Q.; Zhu, M.; Yang, L.; Zhang, J.; Yin, X. The role of land use change in affecting ecosystem services and the ecological security pattern of the Hexi Regions, Northwest China. *Sci. Total Environ.* **2023**, *855*, 158940. [CrossRef] [PubMed]
45. Li, Y.; Liu, W.; Feng, Q.; Zhu, M.; Yang, L.; Zhang, J. Effects of land use and land cover change on soil organic carbon storage in the Hexi regions, Northwest China. *J. Environ. Manag.* **2022**, *312*, 114911. [CrossRef] [PubMed]
46. Peng, S.Z.; Ding, Y.X.; Liu, W.Z.; Li, Z. 1 km monthly temperature and precipitation dataset for China from 1901 to 2017. *Earth Syst. Sci. Data* **2019**, *11*, 1931–1946. [CrossRef]
47. Milly, P.C.D.; Dunne, K.A. Potential evapotranspiration and continental drying. *Nat. Clim. Chang.* **2016**, *6*, 946–949. [CrossRef]
48. Peng, S. *1 km Multi-Scenario and Multi-Model Monthly Temperature Data for China in 2021–2100*; National Tibetan Plateau Data Center: Beijing, China, 2022.
49. Peng, S. *1 km Multi-Scenario and Multi-Model Monthly Precipitation Data for China in 2021–2100*; National Tibetan Plateau Data Center: Beijing, China, 2022.
50. Zhu, M.; Zhang, C.Q.; Zhang, J.T. *30 m Grid Data of 0–100 cm Soil Organic Carbon Density in Qilian Mountains*; National Cryosphere Desert Data Center: Lanzhou, China, 2021.
51. Jiang, T.; Su, B.; Wang, Y.; Wang, G.; Luo, Y.; Zhai, J.Q.; Huang, J.; Jing, C.; Gao, M.; Lin, Q.; et al. Gridded datasets for population and economy under Shared Socioeconomic Pathways for 2020–2100. *Clim. Chang. Res.* **2022**, *18*, 381–383.
52. Xie, G.; Zhang, C.; Zhang, L.; Chen, W.; Li, S. Improvement of the Evaluation Method for Ecosystem Service Value Based on Per Unit Area. *J. Nat. Resour.* **2015**, *30*, 1243–1254.
53. Riahi, K.; van Vuuren, D.P.; Kriegler, E.; Edmonds, J.; O Neill, B.C.; Fujimori, S.; Bauer, N.; Calvin, K.; Dellink, R.; Fricko, O.; et al. The Shared Socioeconomic Pathways and their energy, land use, and greenhouse gas emissions implications: An overview. *Glob. Environ. Chang.* **2017**, *42*, 153–168. [CrossRef]
54. Zhang, S.; Yang, P.; Xia, J.; Wang, W.; Cai, W.; Chen, N.; Hu, S.; Luo, X.; Li, J.; Zhan, C. Land use/land cover prediction and analysis of the middle reaches of the Yangtze River under different scenarios. *Sci. Total Environ.* **2022**, *833*, 155238. [CrossRef]
55. Jiang, C.; Guo, H.; Wei, Y.; Yang, Z.; Wang, X.; Wen, M.; Yang, L.; Zhao, L.; Zhang, H.; Zhou, P. Ecological restoration is not sufficient for reconciling the trade-off between soil retention and water yield: A contrasting study from catchment governance perspective. *Sci. Total Environ.* **2021**, *754*, 142139. [CrossRef] [PubMed]
56. Anselin, L. Local Indicators of Spatial Association-LISA. *Geogr. Anal.* **1995**, *27*, 93–115. [CrossRef]
57. Gaither, C.J.; Poudyal, N.C.; Goodrick, S.; Bowker, J.M.; Malone, S.; Gan, J. Wildland fire risk and social vulnerability in the Southeastern United States: An exploratory spatial data analysis approach. *Forest Policy Econ.* **2011**, *13*, 24–36. [CrossRef]
58. Qian, C.; Gong, J.; Zhang, J.; Liu, D.; Ma, X. Change and tradeoffs-synergies analysis on watershed ecosystem services: A case study of Bailongjiang Watershed, Gansu. *Acta Geogr. Sin.* **2018**, *73*, 868–879.
59. Wang, J.F.; Li, X.H.; Christakos, G.; Liao, Y.L.; Zhang, T.; Gu, X.; Zheng, X.Y. Geographical Detectors-Based Health Risk Assessment and its Application in the Neural Tube Defects Study of the Heshun Region, China. *Int. J. Geogr. Inf. Sci.* **2010**, *24*, 107–127. [CrossRef]
60. Wang, J.F.; Xu, C.D. Geodetector: Principle and prospective. *Acta Geogr. Sin.* **2017**, *72*, 116–134.
61. Li, C.; Wu, X.; Sheridan, S.; Lee, J.; Wang, X.; Yin, J.; Han, J. Interaction of climate and socio-ecological environment drives the dengue outbreak in epidemic region of China. *PLoS Negl. Trop. Dis.* **2021**, *15*, e9761. [CrossRef]
62. Liu, C.; Wang, C.; Li, Y.; Wang, Y. Spatiotemporal differentiation and geographic detection mechanism of ecological security in Chongqing, China. *Glob. Ecol. Conserv.* **2022**, *35*, e2072. [CrossRef]
63. Forthofer, R.N.; Lee, E.S.; Hernandez, M. *13—Linear Regression. Biostatistics (Second Edition)*; Elsevier Inc: Amsterdam, The Netherlands, 2007; pp. 349–386.
64. Zhou, X.; Wen, H.; Zhang, Y.; Xu, J.; Zhang, W. Landslide susceptibility mapping using hybrid random forest with GeoDetector and RFE for factor optimization. *Geosci. Front.* **2021**, *12*, 101211. [CrossRef]
65. Zhao, R.; Zhan, L.; Yao, M.; Yang, L. A geographically weighted regression model augmented by Geodetector analysis and principal component analysis for the spatial distribution of PM2.5. *Sustain. Cities Soc.* **2020**, *56*, 102106. [CrossRef]
66. Wang, B.; Li, X.; Ma, C.F.; Zhu, G.F.; Luan, W.F.; Zhong, J.T.; Tan, M.B.; Fu, J. Uncertainty analysis of ecosystem services and implications for environmental management - An experiment in the Heihe River Basin, China. *Sci. Total Environ.* **2022**, *821*, 153481. [CrossRef] [PubMed]
67. Huang, L.; He, C.; Wang, B. Study on the spatial changes concerning ecosystem services value in Lhasa River Basin, China. *Environ. Sci. Pollut. R* **2022**, *29*, 7827–7843. [CrossRef] [PubMed]
68. Aziz, T. Changes in land use and ecosystem services values in Pakistan, 1950–2050. *Environ. Dev.* **2021**, *37*, 100576. [CrossRef]
69. Qian, D.; Yan, C.; Xiu, L.; Feng, K. The impact of mining changes on surrounding lands and ecosystem service value in the Southern Slope of Qilian Mountains. *Ecol. Complex.* **2018**, *36*, 138–148. [CrossRef]
70. Peng, K.; Jiang, W.; Ling, Z.; Hou, P.; Deng, Y. Evaluating the potential impacts of land use changes on ecosystem service value under multiple scenarios in support of SDG reporting: A case study of the Wuhan urban agglomeration. *J. Clean. Prod.* **2021**, *307*, 127321. [CrossRef]
71. Yang, R.; Ren, F.; Xu, W.; Ma, X.; Zhang, H.; He, W. China's ecosystem service value in 1992–2018: Pattern and anthropogenic driving factors detection using Bayesian spatiotemporal hierarchy model. *J. Environ. Manag.* **2022**, *302*, 114089. [CrossRef]

72. Chen, W.; Chi, G. Ecosystem services trade-offs and synergies in China, 2000–2015. *Int. J. Environ. Sci. Technol.* **2022**, 1–17. [CrossRef]
73. Li, G.; Fang, C.; Wang, S. Exploring spatiotemporal changes in ecosystem-service values and hotspots in China. *Sci. Total Environ.* **2016**, *545–546*, 609–620. [CrossRef]
74. Liu, H.; Zheng, L.; Wu, J.; Liao, Y. Past and future ecosystem service trade-offs in Poyang Lake Basin under different land use policy scenarios. *Arab. J. Geosci.* **2020**, *13*, 46. [CrossRef]
75. Zhang, Z.; Liu, L.; He, X.; Li, Z.; Wang, P. Evaluation on glaciers ecological services value in the Tianshan Mountains, Northwest China. *J. Geogr. Sci.* **2019**, *29*, 101–114. [CrossRef]
76. Pan, J.; Wei, S.; Li, Z. Spatiotemporal pattern of trade-offs and synergistic relationships among multiple ecosystem services in an arid inland river basin in NW China. *Ecol. Indic.* **2020**, *114*, 106345. [CrossRef]
77. Hulvey, K.B.; Mellon, C.D.; Kleinhesselink, A.R. Rotational grazing can mitigate ecosystem service trade-offs between livestock production and water quality in semi-arid rangelands. *J. Appl. Ecol.* **2021**, *58*, 2113–2123. [CrossRef]
78. Shi, M.; Wu, H.; Fan, X.; Jia, H.; Dong, T.; He, P.; Baqa, M.F.; Jiang, P. Trade-Offs and Synergies of Multiple Ecosystem Services for Different Land Use Scenarios in the Yili River Valley, China. *Sustainability* **2021**, *13*, 1577. [CrossRef]
79. Li, J.; Dong, S.; Li, Y.; Wang, Y.; Li, Z.; Li, F. Effects of land use change on ecosystem services in the China–Mongolia–Russia economic corridor. *J. Clean. Prod.* **2022**, *360*, 132175. [CrossRef]
80. Bie, Q.; Xie, Y.W. The constraints and driving forces of oasis development in arid region: A case study of the Hexi Corridor in northwest China. *Sci. Rep.* **2020**, *10*, 17708. [CrossRef]
81. Li, R.; Zheng, H.; Polasky, S.; Hawthorne, P.L.; O Connor, P.; Wang, L.; Li, R.; Xiao, Y.; Wu, T.; Ouyang, Z. Ecosystem restoration on Hainan Island: Can we optimize for enhancing regulating services and poverty alleviation? *Environ. Res. Lett.* **2020**, *15*, 84039. [CrossRef]
82. Wen, Z.; Wu, J.; Yang, Y.; Li, R.; Ouyang, Z.; Zheng, H. Implementing intercropping maintains soil water balance while enhancing multiple ecosystem services. *Catena* **2022**, *217*, 106426. [CrossRef]
83. Wu, J.; Wang, G.; Chen, W.; Pan, S.; Zeng, J. Terrain gradient variations in the ecosystem services value of the Qinghai-Tibet Plateau, China. *Glob. Ecol. Conserv.* **2022**, *34*, e2008. [CrossRef]
84. Kusi, K.K.; Khattabi, A.; Mhammdi, N. Analyzing the impact of land use change on ecosystem service value in the main watersheds of Morocco. *Environ. Dev. Sustain.* **2022**, 1–28. [CrossRef]
85. Fang, J.; Song, H.; Zhang, Y.; Li, Y.; Liu, J. Climate-dependence of ecosystem services in a nature reserve in northern China. *PLoS ONE* **2018**, *13*, e192727. [CrossRef]